Journal of Applied Fluid Mechanics, Vol. 9, No. 6, pp. 3013-3022, 2016.
Available online at www.jafmonline.net, ISSN 1735-3572, EISSN 1735-3645.
DOI: 10.29252/jafm.09.06.26216

Numerical Investigation of the Effect of Corner Radius on Forced Oscillating Square Cylinder

S. Miran[1,2] and C. H. Sohn[2†]

[1] *Department of Mechanical Engineering, University of Gujrat, Gujrat, 50700, Pakistan*
[2] *School of Mechanical Engineering, Kyungpook National University, Daegu, 702-701, Korea,*

†*Corresponding Author Email: chsohn@knu.ac.kr*

(Received February 17, 2016; accepted May 21, 2016)

ABSTRACT

The purpose of this work is to numerically visualize the flow past forced oscillating square cylinder and investigate the effect of corner radius on flow induced forces. The finite volume code was applied to simulate the two dimensional flow past forced oscillating square cylinder with different radius to diameter ratios, (*R/D* = 0 referring to a square cylinder with sharp edges and *R/D* = 0.5 as a circular cylinder). The near wake of a square section cylinder with an increment of *R/D* = 0.1 was studied as the body undergoes a complete oscillatory cycle at lock-in condition, $F = f_e / f_s = 1$ (where f_e is the excitation frequency and f_s is the vortex shedding frequency for the stationary cylinder). The computational model was validated for flow past oscillating cylinder with *R/D* = 0.5 at frequency ratios *F* = 0.5, 1.0 and 1.50, using as the lock-in and lock-out limits and the results shown good agreement. It was observed that computed value of Strouhal Number is nearly same for both stationary and oscillation case and a similar trend was observed, as *R/D* ratio increases. However, the results obtained from oscillation cylinder cases show the significant increase in root mean square value of lift coefficient ($C_{L,RMS}$) and mean drag coefficient (C_D) as compared to the stationary cylinder. Finally, It was found that the percentage increase of $C_{L,RMS}$ is higher than C_D in force oscillating condition for *R/D* = 0, whereas both values decreases with the increase of R/D.

Keywords: Transverse oscillation; Rounded corners; Drag and lift coefficient; Vortex shedding.

NOMENCLATURE

A_m	dimensionless amplitude of the displacement (normalized by *D*)	*R*	radius of corners
		Re	Reynolds number
C_D	drag coefficient	St No.	Strouhal number
C_L	lift coefficient	*t*	non-dimensional time
C_p	pressure coefficient	*T*	period of oscillation
d	normalized boundary distance	*U*	free stream velocity
D	characteristic dimension of cylinder	u, v	velocity components
f_e	excitation frequency	$\vec{u}$	mesh displacement velocity
f_s	frequency of vortex shedding		
F	frequency ratio	α	diffusion parameter
F_D	drag force	γ	diffusion coefficient
F_L	lift force		
p	fluid Pressure		

1. INTRODUCTION

The flow around oscillating bluff bodies has received continued attention over the past few decades due to its wide engineering applications. The vibration arises due to oscillation of cylinder in many practical areas of engineering such as heat exchangers, tubular piles, power cables, marine and wind engineering structures can cause destructive effects on structures. The experimental and numerical studies of the flow around stationary and oscillating circular and square sections have been the center of various investigations over many years. However, some engineering situations demand structural geometries that are neither perfectly square nor circular, but instead are sections with modified corners. For

example, tension leg platforms and semi-submersible drilling rigs used in off-shore engineering applications could have either square or rectangular cross sections with rounded corners. Hence, the study of the flow behavior around such sections is also important where cylinder is not stationary, but oscillates at a certain frequency that could interact with the vortex shedding process. Furthermore, for forced oscillation in a certain range of amplitude and frequency, the cylinder oscillation is able to control the instability mechanism which leads to vortex shedding. The vortex shedding can be controlled by active or passive control methods.

Ongoren and Rockwell (1988) have provided some fundamental investigations in the near wake of oscillating bluff bodies. Luo (1992) studied a transversely oscillating sharp square cylinder and showed the flow field features around it over cycles of oscillation. They reported various modes of vortex shedding at different reduced velocity conditions, but did not consider the corner radius effect. Kwon and Choi (1996) used splitter plates on a circular cylinder to control the vibrations of the cylinders. Bearman and Owen (1998) study the influence of wavy separation lines on a square cylinder using experiments and found that 30% reduction of drag can be achieved when compared with square cylinder.

Tamura *et al*. (1998) has adopted a finite scheme to simulate the flow past a stationary square cylinder with various corner shapes numerically at Re= 10^4. They found that drag could be reduced up to approximately 60% and also observed that the span-wise correlation of fluctuating pressure for rounded corners is larger than for the sharp corners. Further to this, Tamura and Miyagi (1999) have experimentally investigated the influence of the corner effect on 2D and 3D square cylinders both in smooth and in turbulent flows. Blackburn and Henderson (1999) performed 2-D numerical simulations of cross-flow oscillating cylinder at Re = 500 and validated that the change of the lift force on the oscillating cylinder are associated with a change in the timing of the vortex. Zheng and Dalton (1999) have presented an oscillating viscous flow past a square cylinder with square and rounded corners and diamond cylinder with square corners by a finite-difference method. Pavlov *et al*. (2000) carried out two-dimensional (2D) simulation for flow past square cylinder and found that even though 2D numerical results at Re = 500 do not strictly correspond to actual three-dimensional flow, the results remain interesting in their own right due to the simple geometry, rich physical phenomena and relevant practical applications.

Guilmineau and Queutey (2002) numerically simulated transversely oscillating circular cylinders in a uniform flow at fixed Reynolds number equal 185. They have found that when oscillating frequency increases from 0.8 to 1.2, the vortex formation concentration of vortices moves closer to the cylinder until a limiting position. Similarly, Dalton and Zheng (2003) have numerically presented the results for a uniform approach flow for square and diamond sections at Re= 250 and 1000, and observed a considerable effect of corner radius on flow structures for both fixed square and diamond sections. Hu *et al*. (2005) have experimentally investigated the influence of corner radius on the near wake of a stationary square cylinder using PIV and characterize the wake both qualitatively and quantitatively. They found that the leading edge corner radius has more influence in the near wake structure since it determines to a great extent the behavior of the streamlines, the separation angle and the base pressure.

Yang *et al*. (2005) have simulated the flow past a transversely oscillating rectangular cylinder in channel flows. The numerical results captured the flow details at Reynolds number Re = 500. They found that the wake pattern is dominated by the oscillation of the cylinder. Kumar *et al*. (2009) used particle image velocimetry (PIV) technique and found that rounded corners has significantly influenced the flow features around the bodies. Bruneau *et al*. (2012) proposes various active and passive control methods to improve the drag reduction. Singh and Chatterjee (2014) carried out two dimensional numerical investigation to study the effect of transverse shear on freely oscillating circular cylinder at Low Reynolds number and observed the 2S, C(2S) and S + P modes of vortex shedding for various values of *Re* and shear parameters. They found that shear parameter does not effect the maximum displacement but inline displacement is varied while pressure coefficient is also depended on both shear parameter and Reynolds number. Recently, (Miran and Sohn, 2015; Miran and Sohn, 2016) numerically analyzed the effect of rounded corners on the stationary cylinder and found that near wake vortex structures is strongly influenced due to the rounded corner which results of drag and lift force reduction.

Literature indicates that, the numerical simulations with particular focus on an oscillating cylinder flow have been well investigated. However, the aerodynamics behavior and near wake flow features of an oscillating square cylinder with rounded corners is not yet considered in a detailed numerical analysis. In this study, the behavior of time-dependent forces acting on an oscillating square cylinder with different rounded corners are numerically analyzed to give valuable insight into the near wake flow structures of the forced oscillating cylinder and the results are compared with stationary cylinder.

2. COMPUTATIONAL DETAILS

The commercial finite volume code ANSYS Fluent is used to simulate the two dimensional flow past forced transversely oscillating cylinders. The fluid flow is governed by the two dimensional, incompressible, Navier-Stokes equations, which can be expressed as follows:

$$\frac{\partial u}{\partial x}+\frac{\partial v}{\partial y}=0 \tag{1}$$

$$\frac{\partial u}{\partial t}+\frac{\partial u^2}{\partial x}+\frac{\partial uv}{\partial y}=-\frac{\partial p}{\partial x}+\frac{1}{Re}\left(\frac{\partial^2 u}{\partial x^2}+\frac{\partial^2 u}{\partial y^2}\right) \tag{2}$$

$$\frac{\partial v}{\partial t}+\frac{\partial uv}{\partial x}+\frac{\partial v^2}{\partial y}=-\frac{\partial p}{\partial y}+\frac{1}{Re}\left(\frac{\partial^2 v}{\partial x^2}+\frac{\partial^2 v}{\partial y^2}\right) \quad (3)$$

where u and v are the non-dimensional components of the velocity vector in x and y directions, respectively, p is the non-dimensional static pressure, t is the non-dimensional time and Re is the Reynolds number, $Re = \rho UD/\mu$, based on the free stream velocity, U and the characteristic dimension of the body, D.

Figure 1 shows the computational domain and grid system used for the present study. The multiblock technique was used for generation of meshing around the cylinder. In the region around the cylinder wall, fine O-type mesh was used to accurately capture the flow behavior near cylinder walls. In the present study, three different grid sizes (G1-40680, G2-62800, and G3-91530) tests are used to investigate the influence of grid refinement effect on the solution. A detailed mesh independence study has been performed and results are obtained for drag coefficient CD and St. No. The results shown in Table 1 illustrates that there are no considerable changes between G2 and G3. Thus a grid size 62800 (G2) is found to meet the requirements of the both mesh independence and computation time limit. The detail of the influence of the spatial and the temporal resolutions, computational domain independence tests can be found in the published work of Miran and Sohn (2015) for the same configuration and CFD model.

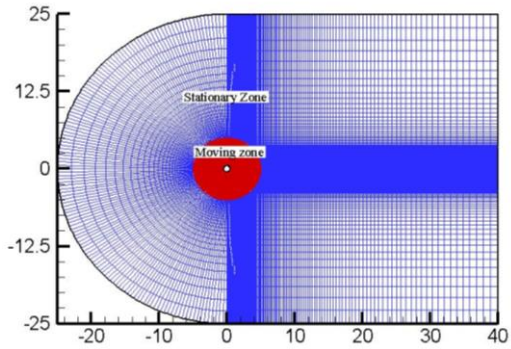

Fig. 1. Computational domain and grid system.

In this study, the diffusion-based mesh smoothing method (Jasak and Tukovic, 2006) based on the algebraic computation of the meshes is used. In order to reduce the computational time the mesh move along with the moving cylinder surface within the 5D zone only (red colour) as shown in Fig 1. Whereas for all other zones, fixed meshes were used. Diffusion based smoothing algorithm moves mesh nodes in response to displacement of boundaries by calculating a mesh velocity using a diffusion equation.

$$\nabla.(\gamma \nabla \vec{u}\,)=0 \quad (4)$$

where $\vec{u}$ is the mesh displacement velocity and γ is the diffusion coefficient. The boundary conditions for Eq. (4) are obtained from the prescribed UDF motion and the diffusion coefficient is used to control how the boundary motion affects the interior mesh motion. The diffusion coefficient as a function of the boundary distance are given in the form of

$$\gamma=\frac{1}{d^{\alpha}} \quad (5)$$

where d is a normalized boundary distance and α is the diffusion parameter. The boundary-distance based diffusion Eq. (5) controls how the boundary motion diffuses into the interior of the domain as a function of boundary distance. In our study, α = 0.5-1 is used as input parameter, to ensure that the value of γ kept near unity to obtain a uniform diffusion of the boundary motion throughout the mesh.

For the forced transversely oscillation, the prescribed motion of the cylinder is given by the excitation frequency and amplitude. The dimensionless transverse cylinder displacement is described by the following harmonic oscillation

$$y(t)=A_m \sin(2\pi f_e t) \quad (6)$$

where $y(t)$ is the dimensionless cylinder displacement at time t, A_m is the dimensionless amplitude of the displacement (normalized by D) and f_e is the excitation frequency of the fixed cylinder.

The boundary conditions adopted for this study consists of the velocity inlet boundary condition with uniform velocity chosen according to D and fluid characteristics (ρ, ν), to obtain the desired Reynolds number, and the outlet boundary set with pressure = 0. No-slip boundary condition was implemented on the cylinder wall and a symmetry boundary condition was imposed to the lateral upper and lower boundaries. The non-dimensional time step Δt = 0.01 was used for all the simulations to ensure that the courant number is less than 1 and convergence is achieved at each time step.

3. RESULTS AND DISCUSSIONS

Simulations are performed for a forced oscillating cylinder at the frequency f_e which is better described by the frequency ratio $F = f_e / f_s$, where f_s is the frequency of vortex shedding. The fixed peak to peak amplitude adopted for forced oscillation is 0.25D for all the cases studied in the present study. The results are validated for force oscillating circular cylinder according to the lock-in and lock-out limits defined by Koopmann (1967). Results obtained for frequency ratios F = 0.5, 1.0 and 1.50 leading to the locked and unlocked wakes are presented in Fig 2. The time histories of lift coefficient for F = 1.0 in Fig 2 shows the pure sinusoidal behavior whereas for F = 0.5 and 1.5 non-regular behavior of oscillating lift and beating phenomenon is observed. Also the power spectral density (PSD) of lift coefficient clearly shows only single peak, which highlight the lock-in condition as $F = f_e / f_s = 1$, and indicates that the fluid forces are now governed by the excitation frequency instead of the Strouhal frequency f_s. The PSD of cases F = 0.5 and 1.5 clearly show the presence of two peaks which identified the unlock behavior of wake. It can also be clearly seen from an analysis of the

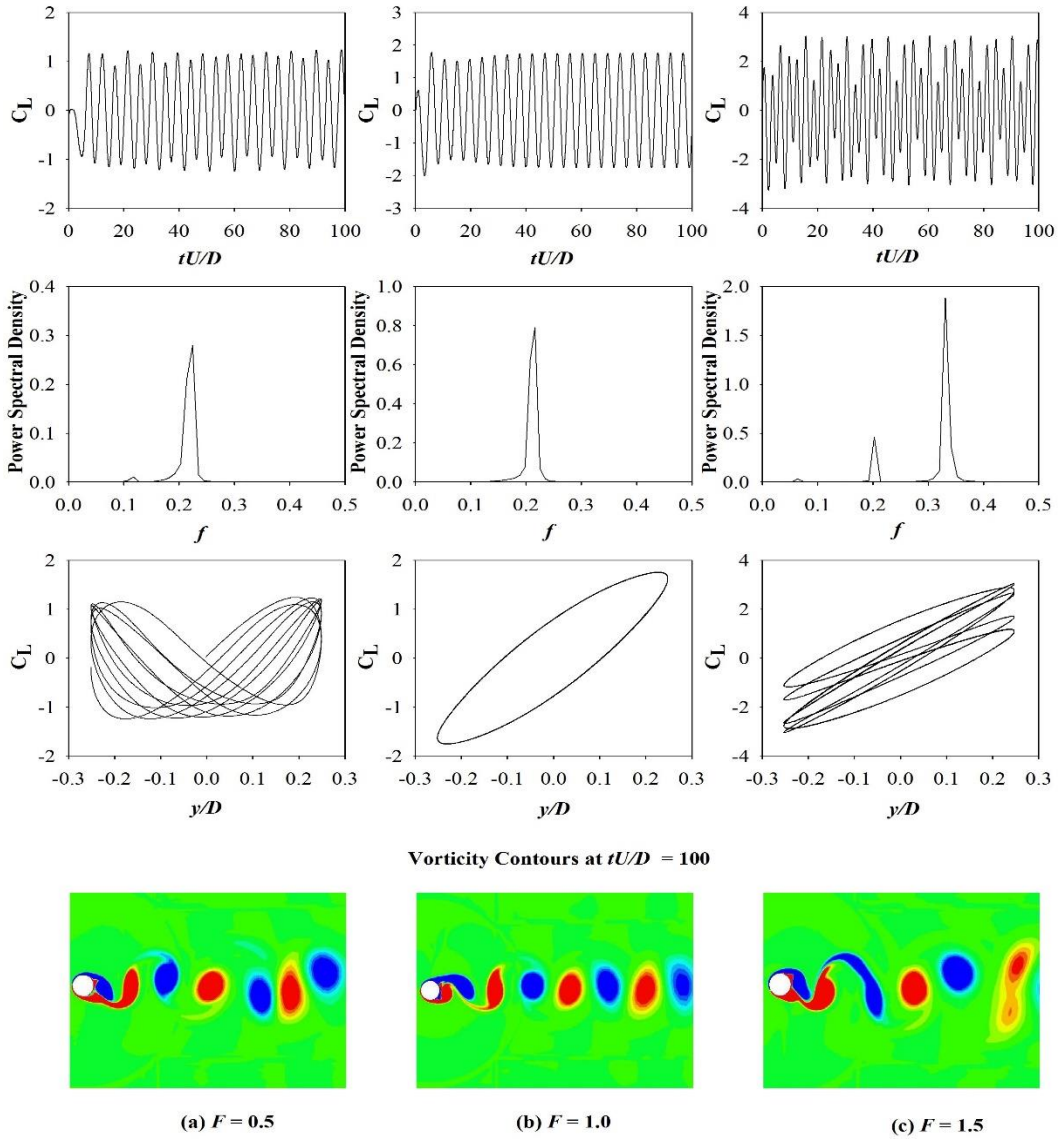

Fig. 2. Time histories of lift coefficient, PSDs of lift coefficient, phase portrait and vorticity contours for *R/D* = 0.5 at *F* = 0.5, 1.0 and 1.5.

phase portraits that single cycle is emerges for lock in wake whereas multiple cycles are observed for lock-out condition. Similarly the vorticity contours presented in Fig 2 also verified the lock-in wake at *F* = 1.0 as the vortices are shed in a regular way, and unlocked wake behavior at *F* = 0.5 and 1.5 as non-regular behavior of vortices shedding. The results presented in Fig 2 have shown good agreement with published results (Bao *et al*., 2012; Placzek *et al*., 2009), which validated our model. After model validation, the near wake of oscillating square cylinder with different, R/D, was studied as the body undergoes a complete oscillatory cycle at lock-in condition *F* = 1.0.

3.1 Instantaneous Vorticity Contours

The instantaneous vorticity contours, during one vortex shedding cycle (*T*) for all the cases with *R/D* = 0-0.5 are shown in Figs 3 to 5. A complete vortex shedding cycle (*T*) is divided into five instantaneous times with equal time intervals, to reveal the variation of the vortex with time: at *t* = 0T the cylinder starts to oscillate from rest; and at *t* = *T/4* the cylinder reaches halfway towards its upward position; at *t* = *T/2* the cylinder reaches at maximum upper position; and at *t* = *3T/4* the cylinder is halfway towards its bottom position of the cylinder; finally at *t* = *T* the cylinder again in its starting position. The vorticity near the upper half of the wake is surrounded with negative vorticity while near the lower wake is surrounded by the positive vorticity. For *R/D* = 0, as the cylinder is forced to move towards the upward position, the positive vortex shedding layer swings upward towards the negative vortex shedding layer and starts to separate from the lower half of the cylinder, and during the first half-cycle of the oscillation vortex pair are shed when cylinder reaches its maximum upward position. Similarly, during the

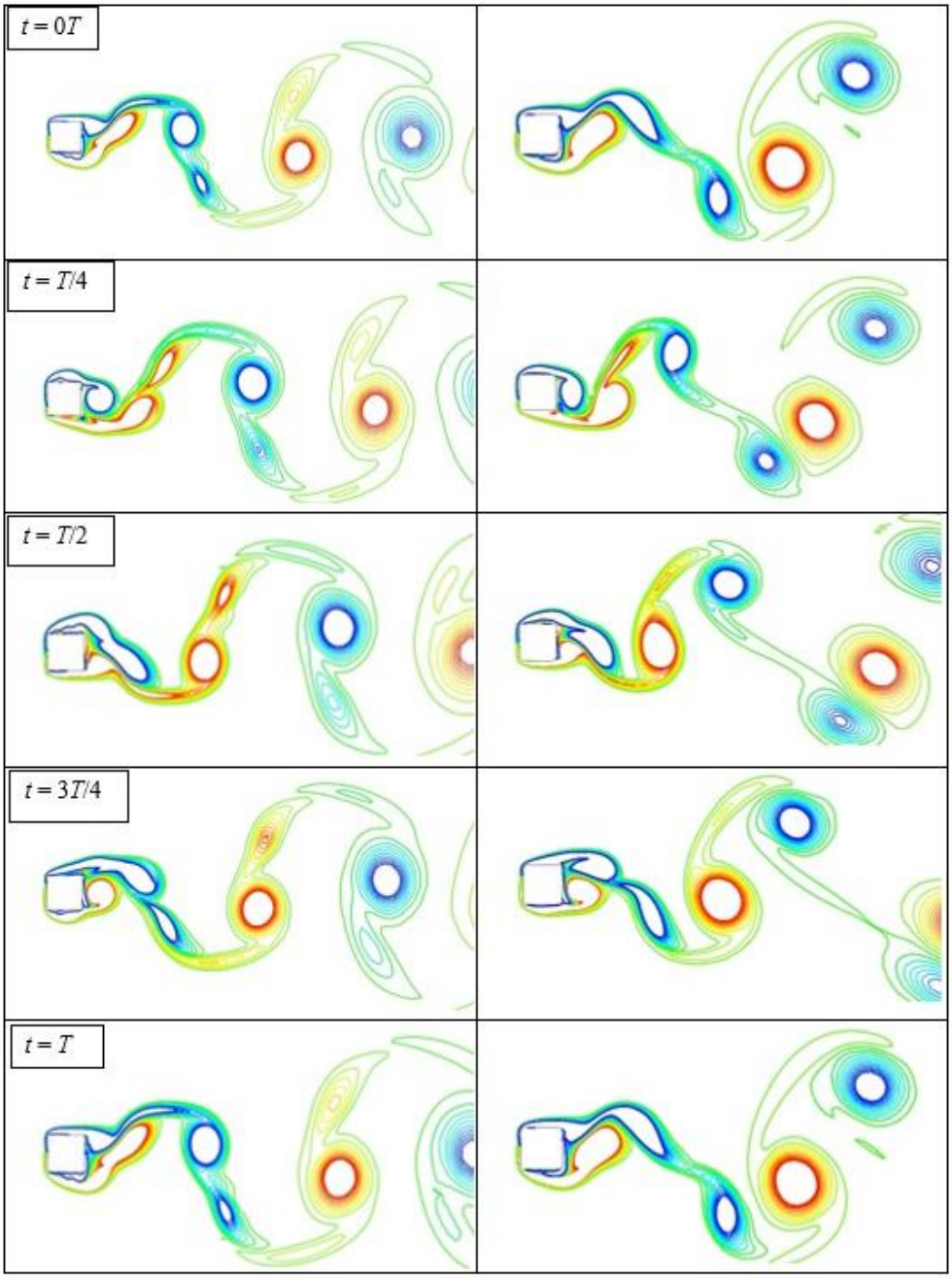

Fig. 3. Instantaneous vorticity contours during one vortex shedding cycle for *R/D* = 0 (left) and 0. 1 (right).

next half cycle when cylinder moves from top to bottom position, the positive pair vortices are shed. The wake pattern is clearly seen to be of 2P-type for square cylinder with sharp corners in Fig 3. Whereas, for *R/D* = 0.1 a single-pair (S+P) vortex are formed during one complete oscillation cycle. However, Fig 4 and 5 showed the mode of vortex shedding for the corner radius ratio R/D = 02-0.5, and is clearly different as compared to *R/D* = 0 and 0.1. For *R/D* = 02-0.5, the vortices are shed in a regular way, which is a result of synchronization of vortex shedding with cylinder motion. As the cylinder approaches upward position, a single negative vortex is shed, and the next half-cycle, the shedding of a single positive vortex, presented the classical Von-Karman Vortex Street, or 2S, mode of shedding. The rounded corner beyond corner radius ratio, *R/D* = 0.2, formed two single vortex (2S) and showed the symmetric pattern. It can also be clearly seen that shear layer is well separated behind corner radius *R/D* = 0-0.1 showed larger fluctuations in the wake than the vortex behind *R/D* = 0.2-0.5 due to which wake width is more and ultimately results the increase of drag.

3.2 Vortex Shedding Frequency

The spectral analysis using Fast Fourier Transform (FFT) was performed on the lift coefficient time history for oscillating cylinder to obtain vortex

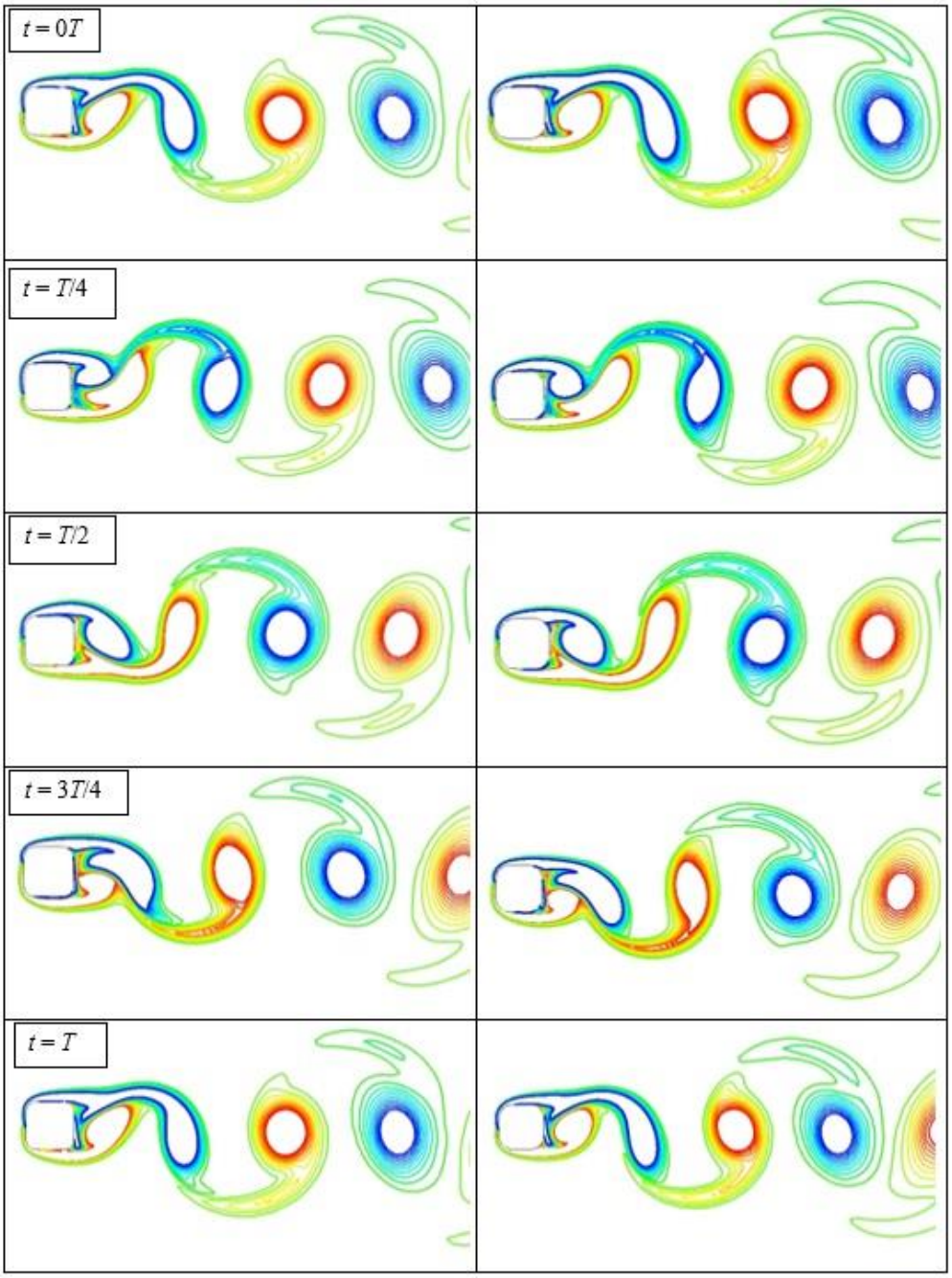

Fig. 4. Instantaneous vorticity contours during one vortex shedding cycle for *R/D* = 0.2 (left) and 0.3 (right).

shedding frequency f_s. The frequency of shedding from the cylinder is normalized as a Strouhal Number, which is defined as, St = f_sD/U. Similarly, the vortex shedding frequency for all rounded corner ratios were obtained for oscillating cases and Strouhal Number (St. No.) was calculated and compared with stationary cases. Fig. 6 illustrates the St. No. for oscillating case and were shown a similar trend to fixed cylinders reported by Miran and Sohn (2015). Also, it can be seen that with the increase of, R/D, the Strouhal Number increases for both cases.

3.3 Drag and Lift Coefficient

The drag and lift forces are usually expressed in non-dimensional forms in terms of C_D and the lift coefficients (C_L) and are given by Eqs. 7 and 8.

$$C_D = \frac{F_D}{0.5\rho U^2 D} \tag{7}$$

$$C_L = \frac{F_L}{0.5\rho U^2 D} \tag{8}$$

where F_D and F_L are the drag and lift forces per unit length, respectively, acting on the cylinder.

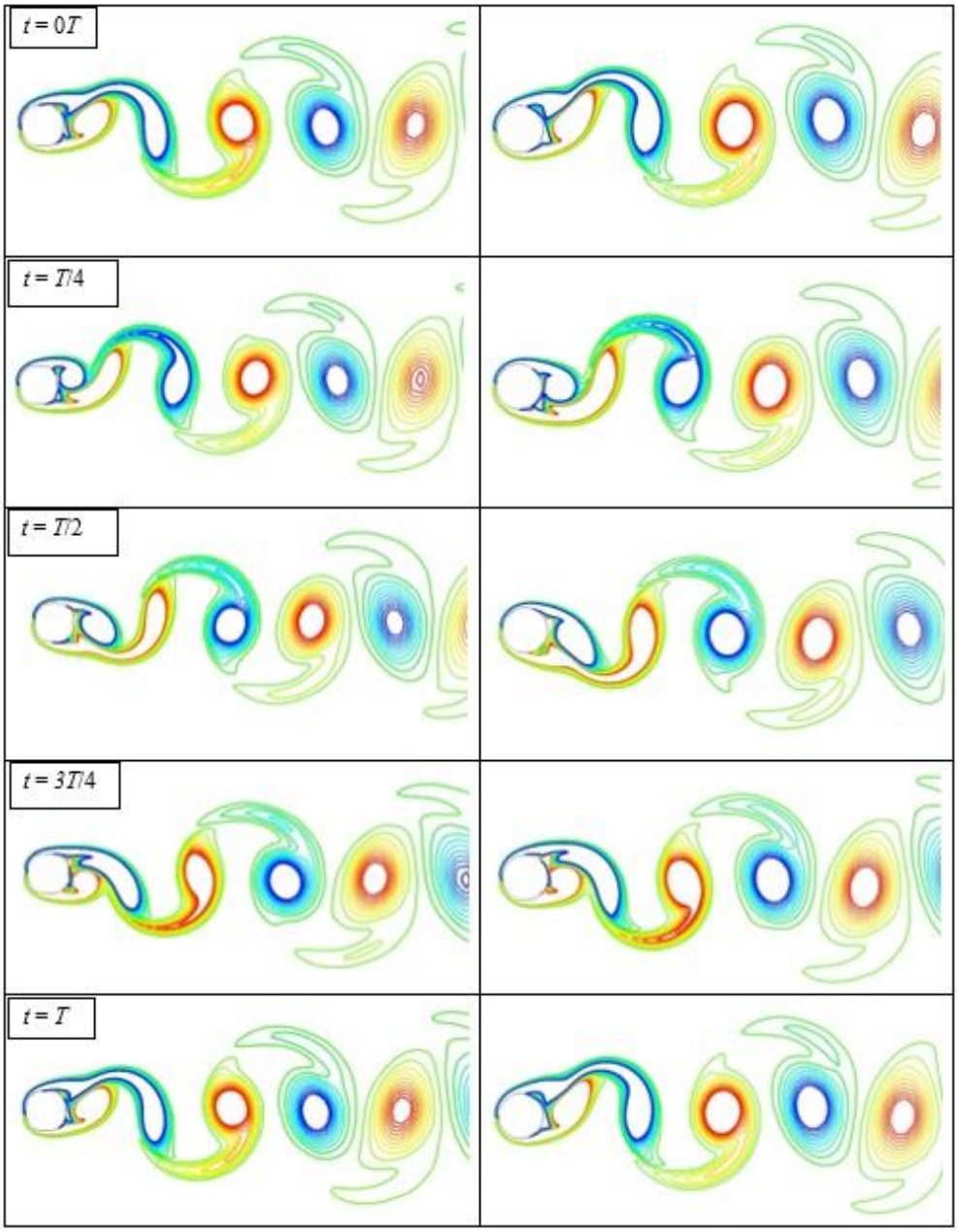

Fig. 5. Instantaneous vorticity contours during one vortex shedding cycle for *R/D* = 0.4 (left) and 0.5 (right).

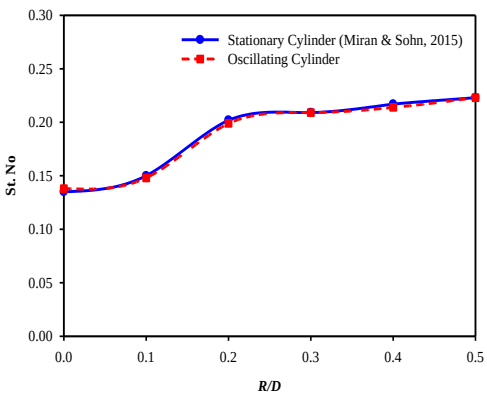

Fig. 6. Variation of Strouhal Number with *R/D*.

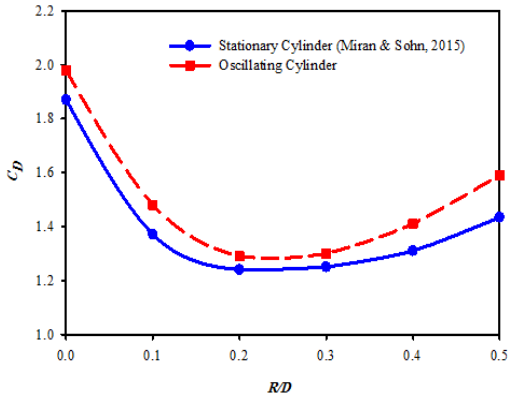

Fig. 7. Variation of mean drag coefficient with *R/D*.

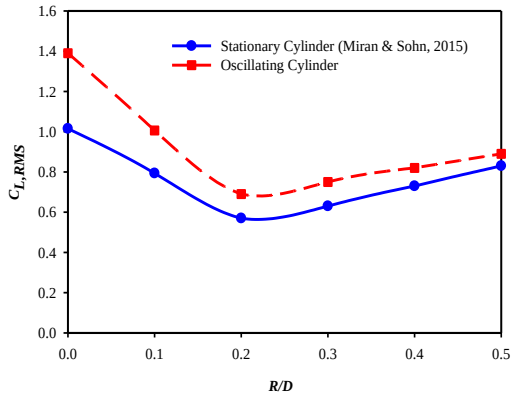

Fig. 8. Variation of root mean square value of lift coefficient with *R/D*.

The RMS value of lift coefficient is obtained by using the following equation.

$$C_{L,RMS} = \sqrt{\frac{1}{N}\sum_{i=1}^{N}(C_{L,i})^2} \quad (9)$$

where $C_{L,i}$ is the instantaneous lift coefficient of a single point in time and N is the number of samples used to calculate the RMS coefficient.

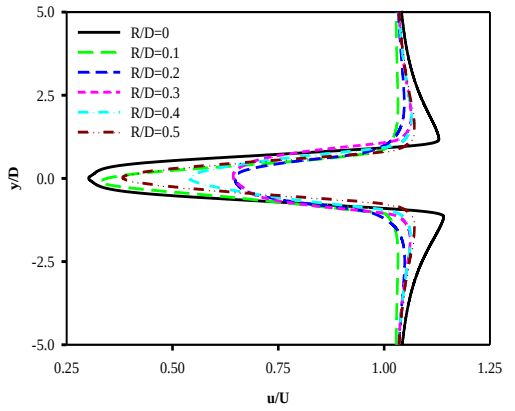

Fig. 9. Time-averaged streamwise velocity profile at *x/D* = 1.5.

Before analyzing the near wake structure of oscillating cylinder, the results of the simulations of flow past a fixed cylinder (Miran and Sohn, 2015) were compared with the present oscillation results to see the effect of oscillation on aerodynamic forces. Mean values for C_D and $C_{L,RMS}$ were obtained by ignoring the initial interval during which the vortex shedding establishes itself and averaging the force time histories of 25 periods of vortex shedding. Fig. 7 shows the mean coefficient of drag C_D both in stationary and oscillating condition. The similar trend was observed for both stationary and oscillation simulation cases, where the minimum C_D is around *R/D* = 0.2 and 0.3, and maximum C_D is *R/D* = 0 for the sharp corner. But percentage increase in C_D is higher in case of oscillation case as compared to the fixed cylinder. From Fig 7, it can be clearly seen that approximately 10 % increase of drag coefficient value was found for transversely oscillating cylinder as compared to stationary cylinder for all *R/D* ratios. As it can be seen from Fig 7 that the cylinders forced to vibrate at lock in condition have substantial increase in drag and can have important consequences for the design of structures.

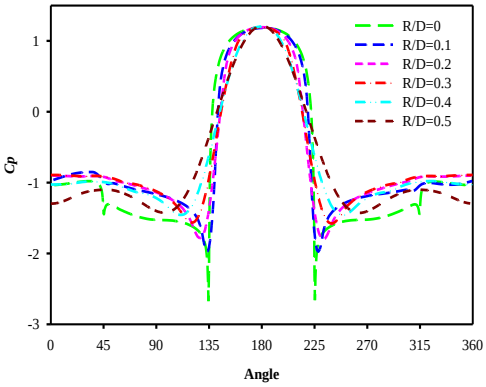

Fig. 10. Mean pressure coefficient for forced oscillation cylinder at different *R/D*.

Table 1 Grid independence study

Grid	Elements	C_D	St. No.	Type of Cylinder
G1	40680	1.821	0.134	Square
G2	62800	1.870	0.135	Square
G3	91530	1.865	0.135	Square

The root mean square value of lift coefficient ($C_{L,RMS}$) for both the stationary and oscillating case are presented in Fig 8. The trend of $C_{L,RMS}$ caused by the effective force of the fluid on the cylinder to oscillate in cross-flow, high $C_{L,RMS}$ means flow induced by force is high. It was observed that $C_{L,RMS}$ has also the similar trend for both cases with *R/D* increases. However, the results show that percentage increase of $C_{L,RMS}$ are higher as compared to C_D in oscillating case. For *R/D* = 0, approximately 40% increase of $C_{L,RMS}$ values were obtained, whereas with the increase of *R/D* value the percentage increase of $C_{L,RMS}$ values decrease and found to be approximately 10% for *R/D* = 0.5. The higher value of $C_{L,RMS}$ is due to forced oscillation of sharp corner cylinder which affects the vortex pattern in the wake.

3.4 Time-Averaged Velocity Profile and Mean Pressure Distribution

Figure 9 illustrates the time-averaged streamwise velocity profiles in the near wake at *x/D* = 1.5 for all rounded corners. The velocity profiles for all *R/D* ratios are symmetric, and illustrate the streamwise decay in the momentum deficit. The *R/D* = 0 gets higher velocity in the center point, whereas *R/D* = 0.2 obtains lower value at the center point. The *u* velocity profile around *R/D* = 0.2-0.3 shows the minimum velocity deficit compared to

other corner radius. This trend is in conformity with the lowest drag and lift coefficient values around *R/D* = 0.2-0.3.

The results for the time averaged pressure distribution obtained for square cylinder with different corner radius are shown in Fig 10. The trend of pressure of stagnation point shown here is in agreement with the trend of C_D and $C_{L,RMS}$, and the time mean minimum pressure point does not change so much from stationary to oscillating. However, the pressure of oscillating case on the rear surface observed here is lower than the stationary case may be because of motion generate additional vortex on the inner shear layer of the rear surface.

4. CONCLUSIONS

Numerical simulation for the forced transverse oscillating cylinders with different *R/D* values were performed for fixed Reynolds number 500 and amplitude 0.25*D* at lock-in condition with finite volume code. The simulation model used in the present is validated and the results have yielded good agreement with the available data. The present results show that physical flow features around the square cylinder in oscillating conditions are strongly influenced by the corner radii. Modes of vortex shedding such as 2S, P+S and 2P are observed for various rounded corners. Results indicate that, as rounded corner ratio increases, the Strouhal Number also increases for oscillating cylinders and have approximately the same value as for stationary cases. However, the calculated values of mean drag coefficient and root mean square value of lift coefficient of the oscillating cases give higher value than the stationary cases. The increase of C_D and $C_{L,RMS}$ for oscillation case is approximately 10% and 40% respectively for sharp corners cylinder. Moreover, the results depict that the value of C_D and $C_{L,RMS}$ in both stationary and oscillating cases were found minimum around R/D = 0.2~0.3.

REFERENCES

Bao, S., S. Chen, Z. Liu, J. Li, H. Wang and C. Zheng (2012). Simulation of the flow around an upstream transversely oscillating cylinder and a stationary cylinder in tandem. *Physics of Fluids 24(2)*, 1-20.

Bearman, P. W. and J. C. Owen (1998). Reduction of bluff-body drag and suppression of vortex shedding by the introduction of wavy separation lines. *Journal of Fluids and Structures 12(1), 123-130*.

Blackburn, H. M. and R. D. Henderson (1999). A study of two-dimensional flow past an oscillating cylinder. *Journal of Fluid Mechanics 385, 255-286*.

Bruneau, C. H., E. Creusé, D. Depeyras, P. Gilliéron and I. Mortazavi (2012). Active and passive flow control around simplified ground vehicles. *Journal of Applied Fluid Mechanics* 5(1), 89-93.

Dalton, C. and W. Zheng (2003). Numerical solutions of a viscous uniform approach flow past square and diamond cylinders. *Journal of Fluids and Structures* 18(3-4), 455-465.

Guilmineau, E. and P. Queutey (2002). A numerical simulation of vortex shedding from an oscillating circular cylinder. *Journal of Fluids and Structures* 16(6), 773-794.

Hu, J. C., Y. Zhou and C. Dalton (2005). Effects of the corner radius on the near wake of a square prism. *Experiments in Fluids* 40(1), 106-118.

Jasak, H. and Z. Tukovic (2006). Automatic mesh motion for the unstructured finite volume method. *Transactions of FAMENA* 30(2), 1-20.

Koopmann, G. (1967). The vortex wakes of vibrating cylinders at low Reynolds numbers. *Journal of Fluid Mechanics* 28(3), 501-512.

Kumar, R. A., C. H. Sohn and B. H. L. Gowda (2009). Influence of corner radius on the near wake structure of a transversely oscillating square cylinder. *Journal of Mechanical Science and Technology* 23(9), 2390-2416.

Kwon, K. and H. Choi (1996). Control of laminar vortex shedding behind a circular cylinder using splitter plates. *Physics of Fluids* 8(2), 479-486.

Luo, S. C. (1992). Vortex wake of a transversely oscillating square cylinder: A flow visualization analysis. *Journal of Wind Engineering and Industrial Aerodynamics* 45(1), 97-119.

Miran, S. and C. H. Sohn (2015). Numerical study of the rounded corners effect on flow past a square cylinder. *International Journal of Numerical Methods for Heat and Fluid Flow* 25(4), 686-702.

Miran, S. and C. H. Sohn (2016). Influence of incidence angle on the aerodynamic characteristics of square cylinders with rounded corners: A numerical investigation. *International Journal of Numerical Methods for Heat and Fluid Flow* 26(1), 269-283.

Ongoren, A. and D. Rockwell (1988). Flow structure from an oscillating cylinder Part 1. Mechanisms of phase shift and recovery in the near wake. *Journal of Fluid Mechanics* 191, 197-223.

Pavlov, A. N., S. S. Sazhin, R. P. Fedorenko and M. R. Heikal (2000). A conservative finite difference method and its application for the analysis of a transient flow around a square prism. *International Journal of Numerical Methods for Heat and Fluid Flow* 10(1), 6-47.

Placzek, A., J. F. Sigrist and A. Hamdouni (2009). Numerical simulation of an oscillating cylinder in a cross-flow at low Reynolds number: Forced and free oscillations. *Computers and Fluids* 38(1), 80-100.

Singh, S. P. and D. Chatterjee (2014). Impact of transverse shear on vortex induced vibrations of

a circular cylinder at low Reynolds numbers. *Computers and Fluids* 93, 61-73.

Tamura, T. and T. Miyagi (1999). The effect of turbulence on aerodynamic forces on a square cylinder with various corner shapes. *Journal of Wind Engineering and Industrial Aerodynamics* 83(1–3), 135-145.

Tamura, T., T. Miyagi and T. Kitagishi (1998). Numerical prediction of unsteady pressures on a square cylinder with various corner shapes. *Journal of Wind Engineering and Industrial Aerodynamics* 74–76, 531-542.

Yang, S. J., T. R. Chang and W. S. Fu (2005). Numerical simulation of flow structures around an oscillating rectangular cylinder in a channel flow. *Computational Mechanics* 35(5), 342-351.

Zheng, W. and C. Dalton (1999). Numerical solutions of a viscous uniform approach flow past square and diamond cylinders. *Journal of Fluids and Structures* 13(2), 225-249.